

REPORT 1088

THEORETICAL DAMPING IN ROLL AND ROLLING MOMENT DUE TO DIFFERENTIAL WING INCIDENCE FOR SLENDER CRUCIFORM WINGS AND WING-BODY COMBINATIONS¹

By GAYNOR J. ADAMS and DUANE W. DUGAN

SUMMARY

A method of analysis based on slender-wing theory is developed to investigate the characteristics in roll of slender cruciform wings and wing-body combinations. The method makes use of the conformal mapping processes of classical hydrodynamics which transform the region outside a circle and the region outside an arbitrary arrangement of line segments intersecting at the origin. The method of analysis may be utilized to solve other slender cruciform wing-body problems involving arbitrarily assigned boundary conditions.

In the present report, the application of the method has shown:

1. That the damping in roll and the rolling moment due to differential incidence of both pairs of opposite surfaces of the cruciform wing-body combinations are practically independent of the body-diameter-maximum-span ratio up to a value of this ratio of 0.3.

2. That the damping in roll of the cruciform wing-body arrangement is only 62 percent greater than that for a corresponding planar wing-body combination.

3. That the rolling moment, resulting from differential incidence of both pairs of the opposing surfaces of the cruciform wing-body arrangement, is only 52 percent greater than that for a corresponding planar wing-body combination.

4. That the rolling effectiveness (wing-tip helix angle per unit surface deflection) of the cruciform wing-body arrangement having four equally deflected panels is therefore 94 percent of the corresponding planar wing-body combination.

INTRODUCTION

Little information is currently available which will permit an evaluation of the stability and control problems associated with the use of cruciform wing and wing-body combinations. In some instances (e. g., the important case of lift), the characteristics of these wings and wing-body combinations may be calculated from known solutions for planar systems, but in other cases the effect of interference between components may be so large as to invalidate the results of such procedures. Additional theoretical treatment is therefore required to establish the magnitude of these interference effects.

An analysis of slender, lifting, planar wing-body and cruciform wing-body combinations was presented by Spreiter in reference 1. Since these results were not applicable to

the present problem, a theoretical investigation of the rolling characteristics of slender cruciform wings was undertaken and reported in reference 2. The present report summarizes these results, and extends the analysis to include slender cruciform wing-body combinations.

Several other analyses of rolling-moment characteristics of cruciform wing and wing-body combinations have been made, each of which partially solves the problem. Ribner (reference 3) has treated the rolling cruciform wing with subsonic leading edges; Bleviss (reference 4) made an analysis for the case of the cruciform wing having supersonic leading edges; Graham (reference 5) has evaluated the rolling moments for cruciform wing-body combinations in the limiting case of an infinite number of fins; and Tucker and Piland (reference 6) have developed a method for obtaining approximate linearized solutions for the damping in roll of wing-body combinations in which the wings have supersonic leading edges, and have calculated the approximate coefficient of damping in roll for configurations having rectangular and triangular wings.

The present analysis considers the case of a slender cruciform wing-body combination consisting of an equal-span cruciform wing mounted on an infinite circular cylinder (fig. 1). The problem will be treated by the well-known methods of slender-wing theory, as introduced by Jones (reference 7) and extended by Ribner and others to determine the aerodynamic characteristics of slender wing and wing-body combinations. In the present report, the method is applied to the determination of the damping in roll and the rolling moment due to differential incidence of one pair of opposite wing panels of a slender cruciform wing-body combination.

The use of slender-wing theory reduces the problem to that of finding the velocity potential defining the two-dimensional flow of an ideal fluid about a finned cylinder; solutions satisfying the prescribed boundary conditions may therefore be obtained by the methods of classical hydrodynamics, in particular, the method of conformal transformation. Since the normal velocity is specified on the boundary, the problem is a Neumann problem in classical potential theory; however, it is convenient to determine the potential by means of a source-sink distribution on the circle in the transformed plane.

¹ Extends the analysis of NACA TN 2270, "Theoretical Damping in Roll and Rolling Effectiveness of Slender Cruciform Wings," by Gaynor J. Adams, 1951.

SYMBOLS

A	aspect ratio $\left(\frac{b_o^2}{S}\right)$
a	body radius
b	local span of wing ($2s$)
b_o	maximum span of wing ($2s_o$)
c_o	chord of wing at plane of symmetry
C_l	rolling-moment coefficient $\left(\frac{L'}{qSb_o}\right)$
C_{l_p}	coefficient of damping in roll $\left(\frac{C_l}{pb_o/2V}\right)$
C_{l_δ}	coefficient of rolling-moment effectiveness $\left(\frac{\partial C_l}{\partial \delta}\right)$
$cn u$ $sn u$	Jacobian elliptic functions, argument u and modulus k
$E(t, k)$	elliptic integral of the second kind, argument t and modulus k
$E(k)$	complete elliptic integral of the second kind, modulus k
$F(t, k)$	elliptic integral of the first kind, argument t and modulus k
$H(u)$	Jacobi's eta function, argument u and modulus k
i	$\sqrt{-1}$
k	modulus of an elliptic integral or function
$K(k)$	complete elliptic integral of the first kind, modulus k
L	lift
L'	rolling moment
m	strength of a point source or sink
M	free-stream Mach number
p	rate of roll, radians per second (constant)
P	loading coefficient $\left(\frac{\Delta p}{q}\right)$
Δp	difference between pressures on lower and upper surfaces
q	free-stream dynamic pressure $\left(\frac{1}{2} \rho V^2\right)$
R	radius of circle in σ plane corresponding to equal-span wing-body surface in X plane $\left(\frac{1}{2} \sqrt{s^2 + \frac{a^4}{s^2}}\right)$
s	local semispan
s_o	maximum semispan
S	area of horizontal surface of cruciform wing including its hypothetical extension through the body
v	velocity component in the y direction
V	free-stream velocity
w	velocity component in the vertical direction
w_o	constant value of w
x, y, z	right-hand orthogonal coordinate system
y_o	value of y corresponding to value of θ_o
X	complex coordinate $(y + iz)$
$Z(A, k)$	Jacobi's zeta function, argument A and modulus k
γ	polar coordinate of the point in the σ plane corresponding to the horizontal wing and body junction in the X plane $\left(\frac{\pi}{4} - \tan^{-1} \lambda^2\right)$
δ	angle of incidence of wing panel, radians ($\delta \ll 1$)
$\Delta \varphi$	$\varphi_l - \varphi_u$
ϵ	semivertex angle of a plane triangular wing
η, ξ	coordinates in the complex ξ plane

θ	polar coordinate in the σ plane
θ_o	angle between a source or sink radius vector and a coordinate axis (σ plane)
Λ	Heuman's form for the incomplete elliptic integral of the third kind
Λ_o	Heuman's form for the complete elliptic integral of the third kind
λ	$\frac{\text{body diameter}}{\text{span}}$
μ	polar coordinate of point in σ plane corresponding to the vertical wing and body junction in the X plane $\left(\frac{\pi}{2} - \gamma\right)$
ξ	complex coordinate $(\eta + i\xi)$
ρ	mass density of air
σ	complex coordinate $(\tau + i\nu)$
τ, ν	coordinates in complex σ plane
f	complex potential $(\varphi + i\psi)$
f_1	complex potential due to a combination of point sources and sinks
φ	velocity potential
ψ	stream function

SUBSCRIPTS

—	value for a plane wing
+	value for a cruciform wing
II	horizontal wing
$L.E.$	value at leading edge
l	value on lower surface
$T.E.$	value at trailing edge
u	value on upper surface
V	vertical wing
γ	value at the point where $\theta = \gamma$

ANALYSIS

GENERAL

Several methods, based on the linearized theory of supersonic flow, have been developed for determining the aerodynamic characteristics of planar-wing systems of finite span. However, the application of these methods to the calculation of the characteristics of a cruciform wing-body combination (fig. 1) leads to considerable mathematical difficulties, since the effects of interference between components cannot be neglected and it is, in general, not practicable to construct solutions from the solutions for planar systems. (An exception is the determination of lift.) It is therefore desirable to introduce simplifying assumptions which permit calculation of the characteristics of cruciform wing-body configurations within reasonable limits of accuracy.

The linearized partial-differential equation for the perturbation velocity potential φ in subsonic and supersonic flow is

$$(1 - M^2) \varphi_{xx} + \varphi_{yy} + \varphi_{zz} = 0 \quad (1)$$

where the free stream is directed parallel to the positive x axis, and M is the free-stream Mach number. If the longitudinal velocity gradient φ_{xx} is sufficiently small and the Mach number is not excessively high, then the first term in equation (1) is small compared to the velocity gradients in

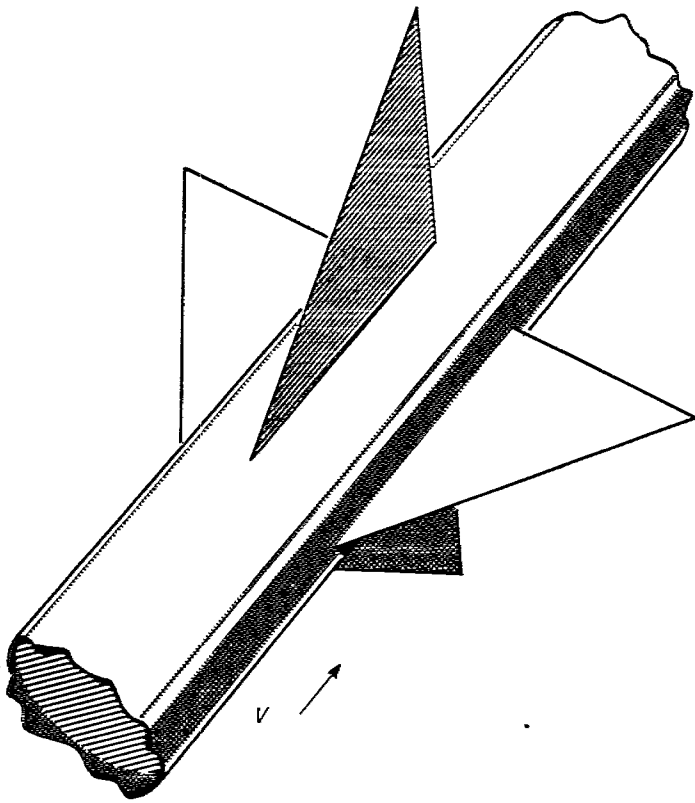


FIGURE 1.—Cruciform wing-body combination.

the y and z directions and may be neglected. Equation (1) then reduces to

$$\varphi_{yy} + \varphi_{zz} = 0 \quad (2)$$

which is the familiar two-dimensional form of Laplace's equation. For slender wings and bodies the velocity gradient φ_{xz} is small, so that a satisfactory approximation to the aerodynamic characteristics of slender wings and wing-body configurations may be obtained by means of equation (2). The results will be independent of Mach number and will be valid for both subsonic and supersonic Mach numbers, as was pointed out in reference 7.

It was pointed out in reference 1, and discussed in greater detail in reference 8, that equation (1) is still valid if M is replaced by unity, in which case equation (1) again reduces to the two-dimensional form of Laplace's equation.

In the present application of the theory, no point on the trailing edge may lie ahead of the most forward point of maximum span. If the latter condition is not satisfied, lift is indicated off the surface of the wing, which violates the boundary conditions. For a more detailed discussion of slender-wing and wing-body theory, the reader is referred to references 1, 7, 8, and 9.

The present problem is solved by finding a solution of equation (2) which satisfies the following boundary conditions:

1. The perturbation velocity components $\frac{\partial \varphi}{\partial y}$ and $\frac{\partial \varphi}{\partial z}$ vanish at infinity.

2. At all points in the $y=0$ or $z=0$ planes (but not on the wing surfaces, or inside the body) $\Delta \varphi = 0$.

3. At all points on the $y=0$ and $z=0$ planes $\Delta \frac{\partial \varphi}{\partial y} = 0$ and $\Delta \frac{\partial \varphi}{\partial z} = 0$, respectively.

4. At all points in the $y=0$ and $z=0$ planes, within the wing plan-form boundaries, $\left(\frac{\partial \varphi}{\partial y}\right)_{y=0}$ and $\left(\frac{\partial \varphi}{\partial z}\right)_{z=0}$, respectively, are specified.

5. At all points on the body surface, $\left(\frac{\partial \varphi}{\partial r}\right)$ is specified.

If the region outside a finned cylinder is mapped conformally on the region outside a circle, with points on the circumference of the circle corresponding to points on the surfaces of the finned cylinder, a potential function satisfying the boundary conditions stated above may be found by integrating a suitable combination of infinitesimal sources and sinks over the circumference of the circle.

If the two-dimensional velocity potential for the flow in transverse planes is given, the local loading coefficient may be written

$$P = \frac{2}{V} \Delta \left(\frac{\partial \varphi}{\partial x}\right) + \frac{1}{V^2} \Delta \left(\frac{\partial \varphi}{\partial y}\right)^2 + \frac{1}{V^2} \Delta \left(\frac{\partial \varphi}{\partial z}\right)^2$$

For this particular problem, the last two terms on the right vanish (cf. boundary conditions above) and the loading coefficient becomes

$$P = \frac{2}{V} \Delta \left(\frac{\partial \varphi}{\partial x}\right) = \frac{4}{V} \frac{\partial \varphi}{\partial s} \frac{ds}{dx} \quad (3)$$

which expresses Bernoulli's equation with the approximation of small disturbances in the case of slender wings and bodies. It follows from equation (3) that the lift of one fin is

$$\left. \begin{aligned} L &= \rho V \int_a^{s_0} dy \int_{L.E.}^{T.E.} \Delta \left(\frac{\partial \varphi}{\partial x}\right) dx \\ &= \rho V \int_a^{s_0} (\Delta \varphi_{T.E.} - \Delta \varphi_{L.E.}) dy \end{aligned} \right\} \quad (4)$$

Similarly, the rolling moment contributed by one fin is

$$L' = -\rho V \int_a^{s_0} (\Delta \varphi_{T.E.} - \Delta \varphi_{L.E.}) y dy \quad (5)$$

In the following section a conformal transformation is derived which maps the region outside a circle on the region outside a cylinder having four fins. It is then shown that, by means of a distribution of infinitesimal sources and sinks on the circumference of the circle, a velocity potential may be found having a normal derivative which satisfies arbitrarily assigned values on the surfaces of the fins.

In succeeding sections the velocity potentials are determined for the cases of a slender, rolling, cruciform wing-body combination and of a slender cruciform wing-body combination for which one pair of fins is differentially deflected through a small angle of incidence. The case where the body radius equals zero (i. e., cruciform wings) is also treated in detail.

CONFORMAL TRANSFORMATION FOR THE CROSS SECTION OF A CRUCIFORM WING-BODY COMBINATION

The transformation of the cruciform wing-body cross section (see fig. 2) may be readily accomplished in two steps. The Joukowski transformation

$$2\xi = X + \frac{a^2}{X} \tag{6}$$

transforms the cruciform wing-body cross section into a cross (fig. 2 (b)) with unequal horizontal and vertical arms; corresponding points are shown in figure 2.

Darwin (reference 10) has given a function which transforms the region outside a circle into the region outside an arbitrary arrangement of line segments intersecting at the origin. By applying Darwin's formula to the cross of figure 2 (b), it is found that the required transformation is

$$2\xi^2 = \sigma^2 + \frac{R^4}{\sigma^2} - 2R^2 \cos 2\mu \tag{7}$$

where R is the radius of the circle in the σ plane, a is the radius of the cylindrical body, and μ is the polar coordinate of the point in the σ plane corresponding to the vertical wing and body junction in the X plane. It can be shown that the vertical and horizontal spans of the cruciform wing-body combination may be taken unequal with no change in the form of equation (7); in this case the radius of the circle is given by the expression

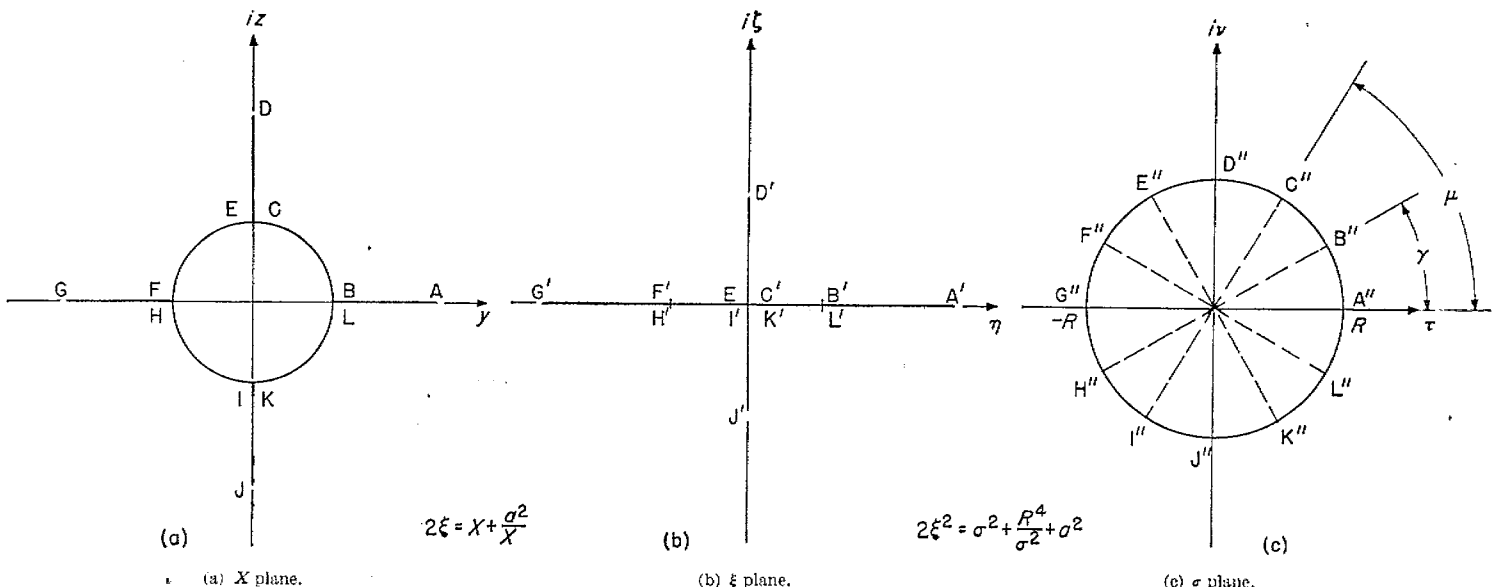
$$8R^2 = s_h^2 + \frac{a^4}{s_h^2} + s_v^2 + \frac{a^4}{s_v^2}$$

where s_h is the semispan of the horizontal wing and s_v is the semispan of the vertical wing. The angles μ and γ are then given by the relations

$$2R^2 \cos 2\mu = \left(s_v^2 + \frac{a^4}{s_v^2}\right) - \left(s_h^2 + \frac{a^4}{s_h^2}\right) - a^2$$

and

$$\cos 2\gamma - \cos 2\mu = \frac{a^2}{R^2}$$



$$2\xi = X + \frac{a^2}{X}$$

$$2\xi^2 = \sigma^2 + \frac{R^4}{\sigma^2} + a^2$$

If $s_h = s_v = s$, equation (7) may be written

$$2\xi^2 = \sigma^2 + \frac{R^4}{\sigma^2} + a^2$$

and from equation (6) and the latter equation it follows that the transformation from the physical plane to the circle is given by

$$X^2 + \frac{a^4}{X^2} = 2 \left(\sigma^2 + \frac{R^4}{\sigma^2} \right) \tag{8}$$

For simplicity, the horizontal and vertical spans have been assumed equal in the present report.

A generalization of equation (8) is

$$X^{n/2} + \frac{a^n}{X^{n/2}} = 2 \left(\sigma^{n/2} + \frac{R^n}{\sigma^{n/2}} \right)$$

where

$$4R^{n/2} = s^{n/2} + \frac{a^n}{s^{n/2}}$$

For a cruciform wing ($a=0$) the equation

$$2X^2 = \sigma^2 + \frac{s^4}{\sigma^2} \tag{9}$$

transforms the equal-span cruciform wing having semispan s into a circle of radius s in the σ plane. A generalization of equation (9) is

$$2X^{n/2} = \sigma^{n/2} + \frac{s^n}{\sigma^{n/2}} \tag{10}$$

where n is a positive integer. Equation (10) maps conformally the region outside a circle $\sigma = se^{i\theta}$ in the σ plane on the region outside a symmetric figure in the X plane, consisting of n line segments of length s having a common point at the origin. This transformation together with the method of this report, may be used to study the rolling-moment characteristics of a slender symmetric wing consisting of n plane fins having a common root chord.

FIGURE 2.—Conformal transformation for the cruciform wing-body combination.

DERIVATION OF THE VELOCITY POTENTIAL

The complex velocity in the physical plane is

$$v - iw = \frac{df}{dX} = \frac{df}{d\xi} \cdot \frac{d\xi}{dX} = (v_\xi - iw_\xi) \frac{d\xi}{dX} \quad (11)$$

Through the use of equation (11) the boundary conditions given in the X plane can be transformed into the corresponding boundary conditions in the ξ plane. The problem is then to find a potential function satisfying these transformed boundary conditions in the transformed plane.

If a source and a sink of strength m are located on the circumference of a circle as shown in figure 3, then the circle is a streamline of the resulting flow. If the flow is transformed into the ξ plane by means of equation (7), the source and sink will be transformed into a "doublet" located in the positive part of the line segment. (See fig. 3 (a).) As shown in this figure, the doublet is characterized by a flow normal to the segment at the point ξ_0 . At all other points on the segments the normal velocity is zero and the segment surfaces are streamlines. In the σ plane the complex potential for the source-sink combination is

$$f_1 = -\frac{m}{2\pi} \log \left(\frac{\sigma - Re^{i\theta_0}}{\sigma - Re^{-i\theta_0}} \right) \quad (12)$$

In the corresponding flow in the ξ plane there is an inflow of $m/2$ units per second above the real axis and an outflow of $m/2$ units per second below the real axis. The flow from an infinitesimal source of strength dm (located on the arc element $Rd\theta_0$ in the σ plane) is, of course, dm units per second. In the ξ plane the flow across the corresponding element

$d\xi_0$ is $|w_\xi d\xi_0|$ units per second, where w_ξ is the vertical velocity component at the point ξ_0 . By the principle of continuity of flow, it is seen that

$$w_\xi d\xi_0 = \frac{dm}{2} \quad (13)$$

where w_ξ may be any function of ξ_0 , and $d\xi_0$ is obtained from equation (7). The complex potential corresponding to any assigned distribution of w_ξ may then be found by replacing m by dm in equation (12) and integrating over the proper range of values of ξ_0 . This procedure will be followed in the succeeding sections.

It is evident from the preceding discussion that the present method of analysis may also be applied to nonsteady flow problems by making the doublet strength a function of time.

APPLICATIONS

ROLLING MOMENT DUE TO ROLLING

Equal-span cruciform wing-body combination.—The case of a slender equal-span cruciform wing-body combination rolling about its longitudinal axis with constant angular velocity p will now be considered. The complex potential for the source-sink combination shown in figure 4 is

$$f_1 = -\frac{m}{2\pi} \log \left(\frac{\sigma^4 - R^4 e^{4i\theta_0}}{\sigma^4 - R^4 e^{-4i\theta_0}} \right)$$

Replacing m by $dm = 2w dy_0 = -2 \frac{\partial \psi}{\partial y_0} dy_0 = -2d\psi$, and integrating from $\theta_0 = 0$ to $\theta_0 = \gamma$, the complex potential is

$$f = \frac{1}{\pi} \int_{\theta_0=0}^{\theta_0=\gamma} \log \left(\frac{\sigma^4 - R^4 e^{4i\theta_0}}{\sigma^4 - R^4 e^{-4i\theta_0}} \right) d\psi$$

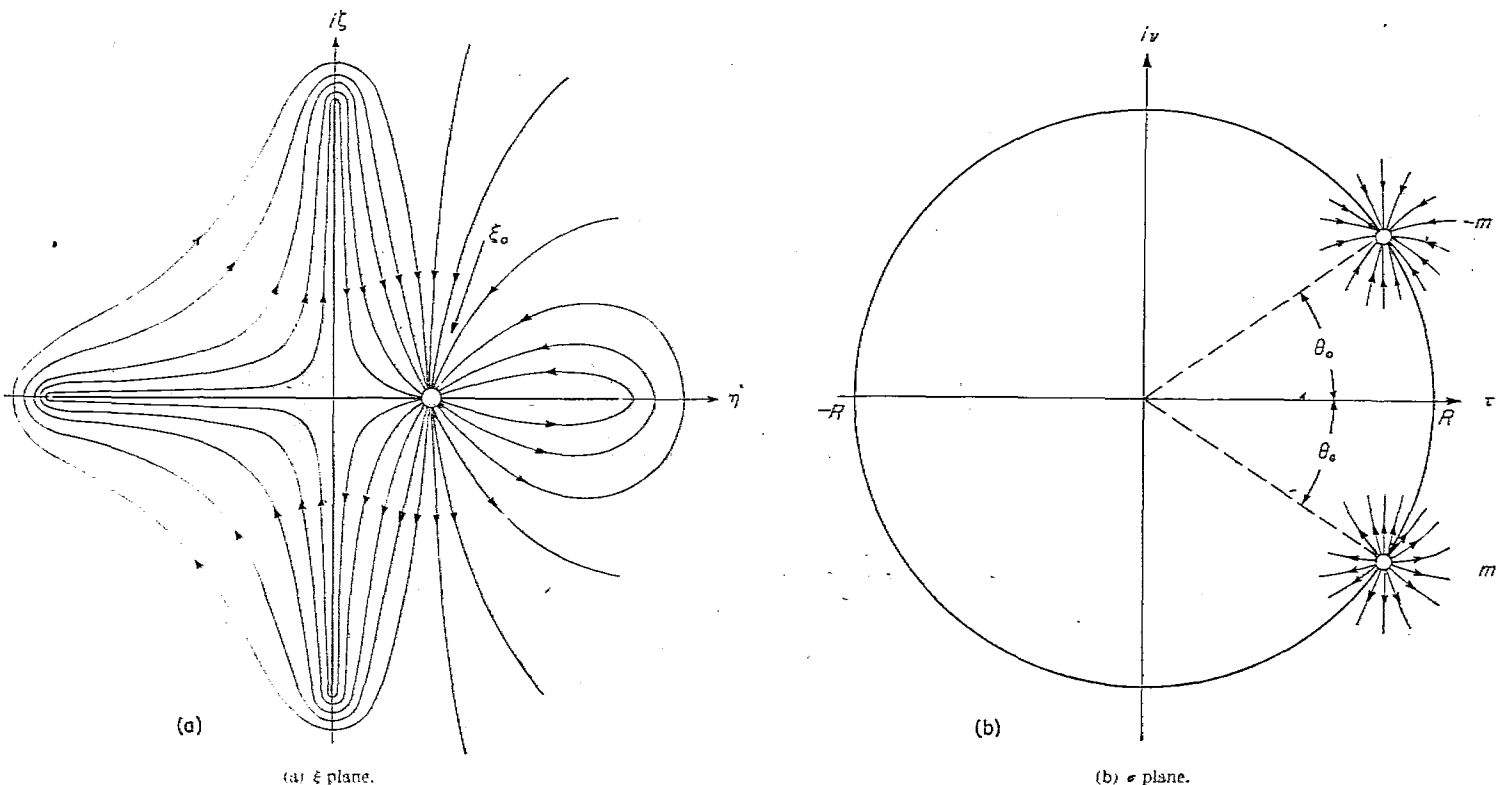


FIGURE 3.—Doublet flow in ξ plane corresponding to source-sink flow in σ plane.

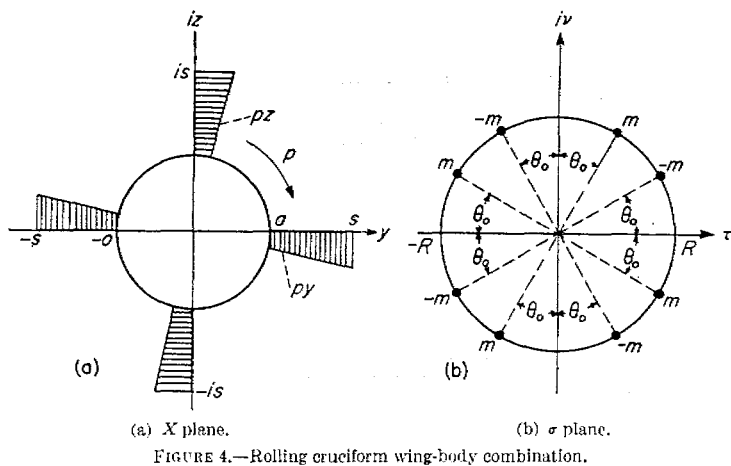


FIGURE 4.—Rolling cruciform wing-body combination.

Integrating by parts yields

$$f = \frac{\psi_\gamma}{\pi} \log \left(\frac{\sigma^4 - R^4 e^{4i\gamma}}{\sigma^4 - R^4 e^{-4i\gamma}} \right) - \frac{4i}{\pi} (R^8 - \sigma^8) \int_0^\gamma \frac{\psi(\theta_0) d\theta_0}{\sigma^8 + R^8 - 2R^4 \sigma^4 \cos 4\theta_0} \quad (14)$$

where an imaginary constant has been omitted. Substituting $\sigma = R e^{i\theta}$ into equation (14), and evaluating the real part yields for the surface velocity potential

$$\varphi = \frac{\psi_\gamma}{\pi} \log \left| \frac{\sin 2(\gamma - \theta)}{\sin 2(\gamma + \theta)} \right| - \frac{4}{\pi} \sin 4\theta \int_0^\gamma \frac{\psi(\theta_0) d\theta_0}{\cos 4\theta - \cos 4\theta_0} \quad (15)$$

for all values of θ ($-\pi \leq \theta \leq \pi$). Equation (15) gives the velocity potential for any symmetric distribution of normal velocity components on the fins of an equal-span cruciform wing-body configuration. The principal value of the integral must, of course, be taken if $\cos 4\theta = \cos 4\theta_0$ in the interval of integration. For the present problem ψ is equal to $\frac{1}{2} p y_0^2$ on the real axis (it is assumed that the unsteady flow condition is approximated by fins with linear twist) and from equation (8)

$$\frac{y_0}{R} = \sqrt{\cos 2\theta_0 - \cos 2\gamma} + \sqrt{\cos 2\theta_0 + \cos 2\gamma} \quad (16)$$

Substitution of these equations into equation (15) yields

$$\varphi = \frac{p a^2}{2\pi} \log \left| \frac{\sin 2(\gamma - \theta)}{\sin 2(\gamma + \theta)} \right| - \frac{4p R^2}{\pi} \sin 4\theta \int_0^\gamma \frac{\cos 2\theta_0 d\theta_0}{\cos 4\theta - \cos 4\theta_0} - \frac{4p R^2}{\pi} \sin 4\theta \int_0^\gamma \frac{\sqrt{\cos^2 2\theta_0 - \cos^2 2\gamma}}{\cos 4\theta - \cos 4\theta_0} d\theta_0 \quad (17)$$

Evaluation of the integrals in equation (17) yields for the surface velocity potential on the horizontal wing surface

$$\varphi_H = \pm \frac{2p R^2}{\pi} \left[\cos 2\theta \tanh^{-1} \left(\frac{\sin 2\theta}{\sin 2\gamma} \right) - \cos 2\gamma \tanh^{-1} \left(\frac{\tan 2\theta}{\tan 2\gamma} \right) \right] \pm \frac{p R^2}{\pi} [K(k_1) \sin 4\theta - 2k_1 \cos A_1 K(k_1) Z(A_1, k_1)] \quad (18)$$

where

$$k_1 = \sin 2\gamma$$

$$A_1 = \sin^{-1} \left(\frac{\sin 2\theta}{\sin 2\gamma} \right)$$

and Z is Jacobi's zeta function. The derivative of φ_H with respect to s is

$$\frac{\partial \varphi_H}{\partial s} = \frac{\partial \varphi_H}{\partial R} \frac{\partial R}{\partial s} + \frac{\partial \varphi_H}{\partial \gamma} \frac{\partial \gamma}{\partial s} + \frac{\partial \varphi_H}{\partial \theta} \frac{\partial \theta}{\partial s} \quad (19)$$

From equations (3), (18), and (19) it follows that the loading on a spanwise strip for the slender, rolling cruciform wing-body combination is given by

$$\frac{1}{(1 + \lambda^4) \left(\frac{pb}{2V} \right) \frac{ds}{dx}} P = \frac{4}{\pi} \left\{ \frac{k_1 [k_1 + E(k_1)]}{\tan 2\theta} + \frac{k_1'^2 K(k_1) Z(A_1, k_1)}{\cos A_1} \right\} \quad (20)$$

This load distribution is shown in figure 5.

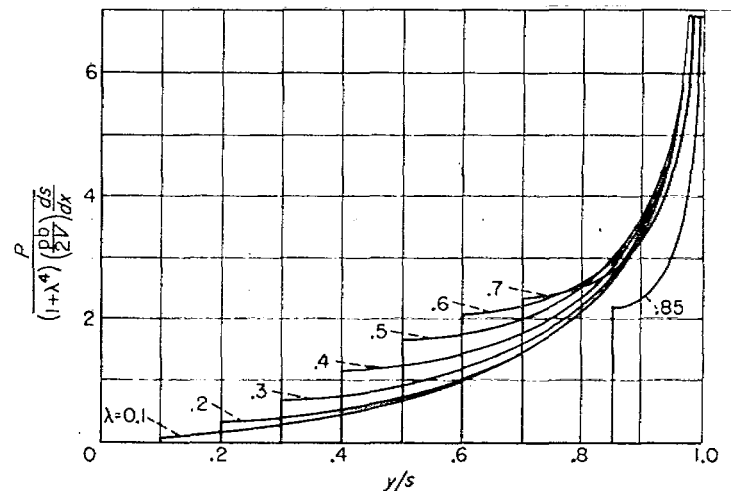


FIGURE 5.—Load distributions on spanwise strips for rolling cruciform wing-body combinations.

The rolling moment due to rolling for each fin may be found by substituting equation (18) into equation (5) and integrating. The results, as obtained by numerical integration, are presented in coefficient form in figure 6, as a function of body-diameter-maximum-span ratio. The area used in defining the aspect ratio and the moment coefficient is the area of the horizontal surfaces of the cruciform wing, including its hypothetical extension through the body. For purposes of comparison, figure 6 includes the coefficient of damping in roll for a slender planar wing body as given in reference 12. It is evident that for these cases the body has little effect on the damping moment up to $\lambda = 0.4$.

Equal-span cruciform wing.—If a is placed equal to zero ($\lambda = \pi/4$, $R = s/2$) then equation (18) reduces to

$$\varphi_H = \pm \frac{p}{\pi} y^2 \operatorname{sech}^{-1} \left(\frac{y}{s} \right)^2 \quad (21)$$

which agrees with the result given in references 2 and 3 for the surface velocity potential of a rolling cruciform wing. Similarly, equation (20) reduces to

$$\frac{1}{\left(\frac{pb}{2V} \right) \frac{ds}{dx}} P = \frac{8}{\pi} \frac{(y/s)^2}{\sqrt{1 - (y/s)^4}} \quad (22)$$

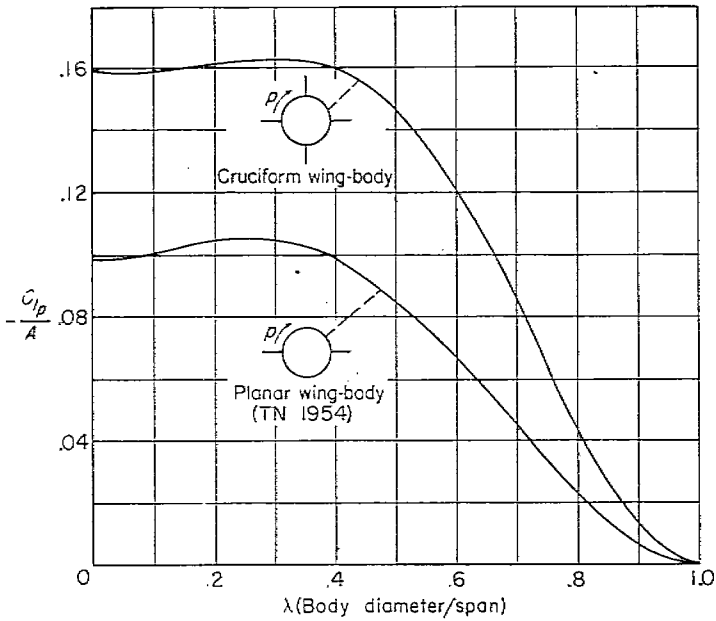


FIGURE 6.—Coefficient of damping in roll for cruciform and planar wing-body combinations.

If the velocity potential for a slender, rolling planar wing (reference 13) is substituted into equation (3), it is found that the loading on a spanwise strip is given by

$$\left(\frac{pb}{2V}\right) \frac{ds}{dx} P_- = \frac{2(y/s)}{\sqrt{1-(y/s)^2}} \quad (23)$$

Figure 7, which presents these load distributions, shows the effect of the wing interference in reducing the load distribution which opposes the rolling motion.

Substituting equation (21) into equation (5) yields the total rolling moment due to roll for a slender cruciform wing

$$(L')_{\pm} = -\frac{8\rho V p}{\pi} \int_0^{s_0} y^3 \operatorname{sech}^{-1}\left(\frac{y}{s_0}\right)^2 dy$$

$$= -\frac{2}{\pi} \rho V p s_0^4$$

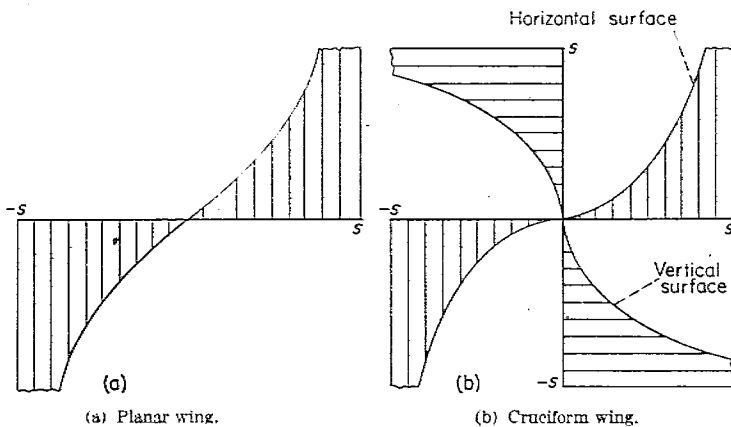


FIGURE 7.—Load distributions on a spanwise strip for rolling wings.

The coefficient of damping in roll is therefore simply

$$(C_{i_p})_+ = -\frac{2 \tan \epsilon}{\pi}$$

$$= -\frac{A}{2\pi}$$

where the coefficient is based on the area of the horizontal wing only.

For a slender planar wing it is known (reference 13) that the coefficient of damping in roll is

$$(C_{i_p})_- = -\frac{\pi \tan \epsilon}{8}$$

$$= -\frac{\pi A}{32}$$

The ratio of the damping moments for the rolling cruciform wing and the rolling planar wing is therefore

$$\frac{(L')_+}{(L')_-} = \frac{16}{\pi^2} = 1.62$$

The damping in roll for the slender cruciform wing is therefore only 62 percent greater than that for a planar wing having the same aspect ratio.

ROLLING MOMENT DUE TO DIFFERENTIAL WING INCIDENCE

Equal-span cruciform wing-body combination.—The case considered here consists of a slender, equal-span, cruciform wing-body combination in which the horizontal fins are differentially deflected through a small angle δ . The vertical velocity component on the surface of each horizontal fin is constant, and is $w_0 = \pm V\delta$; on the surfaces of the vertical fins the lateral velocity component must be zero, and the radial velocity component on the body surface must be zero.

The complex potential for the source-sink combination shown in figure 8 is

$$f_1 = -\frac{m}{2\pi} \log\left(\frac{\sigma^2 - R^2 e^{2i\theta_0}}{\sigma^2 - R^2 e^{-2i\theta_0}}\right)$$

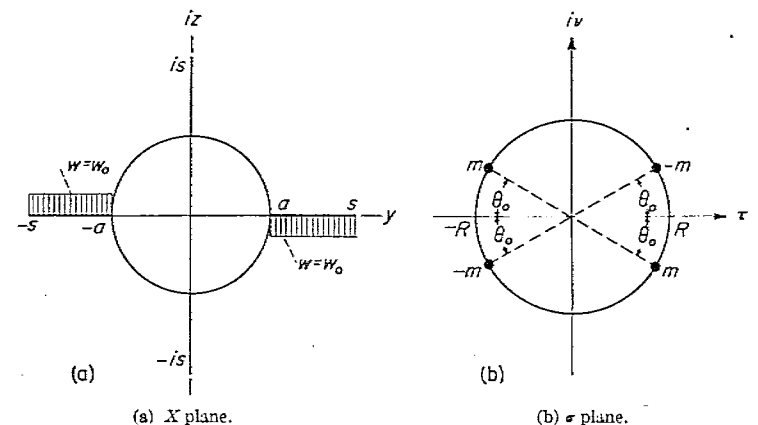


FIGURE 8.—Cruciform wing-body combination with differential incidence of the horizontal surfaces.

Replacing m by $dm = 2w dy_o = -2 \frac{\partial \psi}{\partial y_o} dy_o = -2d\psi$, and integrating from $\theta_o = 0$ to $\theta_o = \gamma$, the complex potential is

$$f = \frac{1}{\pi} \int_{\theta_o=0}^{\theta_o=\gamma} \log \left(\frac{\sigma^2 - R^2 e^{2i\theta_o}}{\sigma^2 - R^2 e^{-2i\theta_o}} \right) d\psi$$

Integration by parts yields

$$f = \frac{\psi_\gamma}{\pi} \log \left(\frac{\sigma^2 - R^2 e^{2i\gamma}}{\sigma^2 - R^2 e^{-2i\gamma}} \right) - \frac{2i}{\pi} (R^4 - \sigma^4) \int_0^\gamma \frac{\psi(\theta_o) d\theta_o}{\sigma^4 + R^4 - 2R^2 \sigma^2 \cos 2\theta_o} \quad (24)$$

where an imaginary constant has been omitted. Substituting $\sigma = R e^{i\theta}$ into equation (24), and evaluating the real part yields for the surface velocity potential

$$\varphi = \frac{\psi_\gamma}{\pi} \log \left| \frac{\sin(\gamma - \theta)}{\sin(\gamma + \theta)} \right| - \frac{2}{\pi} \sin 2\theta \int_0^\gamma \frac{\psi(\theta_o) d\theta_o}{\cos 2\theta - \cos 2\theta_o} \quad (25)$$

for all values of θ ($-\pi \leq \theta \leq \pi$). Equation (25) gives the surface velocity potential for a cruciform wing-body combination having any specified antisymmetric distribution of the vertical velocity component on the horizontal surfaces. The principal value of the integral must, of course, be taken if θ is such that $\cos 2\theta = \cos 2\theta_o$ in the interval of integration.

For the present problem ψ is equal to $w_o y_o$ on the real axis; substitution of this equation and equation (16) into equation (25) yields

$$\varphi = \frac{w_o a}{\pi} \log \left| \frac{\sin(\gamma - \theta)}{\sin(\gamma + \theta)} \right| - \frac{2w_o R}{\pi} \sin 2\theta \int_0^\gamma \frac{\sqrt{\cos 2\theta_o - \cos 2\gamma}}{\cos 2\theta - \cos 2\theta_o} d\theta_o - \frac{2w_o R}{\pi} \sin 2\theta \int_0^\gamma \frac{\sqrt{\cos 2\theta_o + \cos 2\gamma}}{\cos 2\theta - \cos 2\theta_o} d\theta_o \quad (26)$$

for the surface velocity potential for the cruciform wing-body configuration with differential incidence of the horizontal surfaces. By replacing the upper limit in the integral of equation (26) by an appropriate value determined from equation (8), the velocity potential may be obtained for a cruciform wing-body combination having differential incidence of the outer portions of the horizontal fins.

The first and second integrals occurring in equation (26) are complete and incomplete elliptic integrals of the third kind, respectively; these integrals may be reduced to Jacobi's normal form by the respective elliptic substitutions

$$\sin \theta_o = \sin \gamma \operatorname{sn}(u, k_2); \quad k_2 = \sin \gamma$$

$$\sin \theta_o = \cos \gamma \operatorname{sn}(u, k_3); \quad k_3 = \cos \gamma$$

The surface velocity potential may then be written in the form

$$\varphi = \frac{w_o a}{\pi} \log \left| \frac{\sin(\gamma - \theta)}{\sin(\gamma + \theta)} \right| - \frac{2w_o R}{\pi} (I_1 + I_2) \sin 2\theta \quad (27)$$

where

$$I_1 = \frac{k_2^2}{\sqrt{2}} \int_0^{K(k_2)} \frac{cn^2 u du}{k_2^2 sn^2 u - \sin^2 \theta}; \quad sn u \equiv sn(u, k_2)$$

$$I_2 = \frac{k_3^2}{\sqrt{2}} \int_0^{sn^{-1}(\tan \gamma)} \frac{cn^2 u du}{k_3^2 sn^2 u - \sin^2 \theta}; \quad sn u \equiv sn(u, k_3)$$

Equation (27) gives the surface velocity potential for all values of θ ($-\pi \leq \theta \leq \pi$); the explicit evaluation of the integrals, of course, depends upon the range of values of the parameters occurring in the integrands (references 14 and 15).

Evaluation of the integrals in equation (27) for $z = 0$, $a \leq y \leq s$ (horizontal fin, positive real axis) yields

$$\left. \begin{aligned} I_1 &= -\frac{1}{\sqrt{2}} \left[K(k_2) - 2k_2 \left(\frac{\cos A_2}{\sin 2\theta} \right) K(k_2) Z(A_2, k_2) \right] \\ I_2 &= -\frac{F(A_3, k_3)}{\sqrt{2}} \left\{ 1 - 2k_3 \left(\frac{\cos A_4}{\sin 2\theta} \right) [Z(A_4, k_3) - G] \right\} \end{aligned} \right\} \quad (28)$$

where

$$\begin{aligned} A_2 &\equiv \sin^{-1} \left(\frac{\sin \theta}{\sin \gamma} \right) \\ A_3 &\equiv \sin^{-1} (\tan \gamma) \\ A_4 &\equiv \sin^{-1} \left(\frac{\sin \theta}{\cos \gamma} \right) \\ G &\equiv \frac{1}{2F(A_3, k_3)} \log \frac{H[F(A_3, k_3) + F(A_4, k_3)]}{H[F(A_3, k_3) - F(A_4, k_3)]} \end{aligned}$$

and the modulus of H is k_3 .

Equations (27) and (28) define the surface velocity potential φ_H on the deflected surfaces of the cruciform wing-body combination.

For values of θ corresponding to points on the vertical surfaces, integration of equation (27) yields

$$\left. \begin{aligned} I_1 &= -\frac{1}{\sqrt{2}} \left\{ \frac{k_2^2 K(k_2)}{\sin^2 \theta} - \frac{\pi \sqrt{\sin^2 \theta - \sin^2 \gamma}}{\sin 2\theta} [1 - \Lambda_o(A_5, k_2)] \right\} \end{aligned} \right\} \quad (29)$$

where

$$A_5 \equiv \sin^{-1} \left(\frac{\sqrt{\cos^2 \gamma - \cos^2 \theta}}{\cos \gamma \sin \theta} \right)$$

and Λ_o is Heuman's form (reference 16) for the complete elliptic integral of the third kind. The second integral is

$$I_2 = -\frac{1}{\sqrt{2}} \left[F(A_3, k_3) - \frac{2k_2 \cos A_6}{\sin 2\theta} \Lambda(\mu, A_6, A_3) \right] \quad (30)$$

where

$$A_6 \equiv \sin^{-1} \left(\frac{\cos \theta}{\sin \gamma} \right)$$

and Λ is Heuman's form for the incomplete elliptic integral of the third kind.

Equations (27), (29), and (30) define the surface velocity potential φ_V on the vertical surfaces of the cruciform wing-body combination with differential incidence of the horizontal surfaces.

The rolling moment due to differential incidence of one pair of fins may be found by substituting the preceding equations for φ_H and φ_V in equation (5) and integrating. The results, obtained by numerical integration, are presented in coefficient form in figures 9 and 10 as functions of λ . The aspect ratio and coefficients are based on the area of the horizontal surfaces of the cruciform wing, including its hypothetical extension through the body.

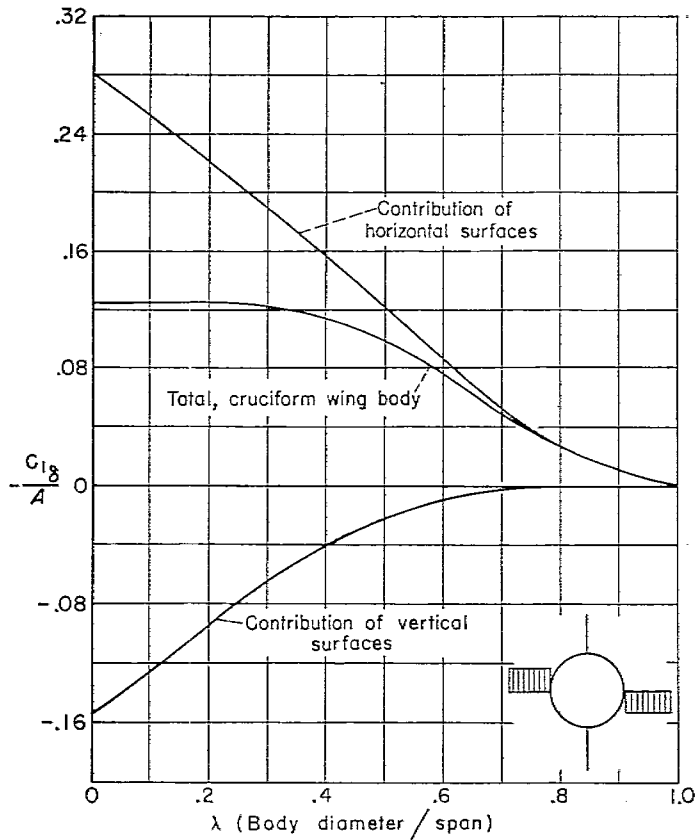


FIGURE 9.—Coefficient of rolling-moment effectiveness for cruciform wing-body combinations with differential incidence of the horizontal surfaces.

Figure 9 gives the coefficients of rolling-moment effectiveness for both the deflected and the undeflected surfaces, as well as their algebraic sum, that is, the total rolling-moment effectiveness for the configuration. Figure 10 also gives the coefficient of rolling-moment effectiveness for a slender planar wing-body combination with differential incidence of the wing surfaces; the velocity potential for this case was derived by mapping the configuration cross section on a circle by means of two successive applications of the Joukowski transformation, that is,

$$2\xi = X + \frac{a^2}{X}; 2\xi = \sigma + \frac{s_1^2}{\sigma}$$

where the X plane is the physical plane and the wing-body cross section is transformed into a circle of radius s_1 in the σ plane. The velocity potential on the wing surface is given by

$$\frac{\varphi_w}{V\delta s_1} = \frac{2}{\pi} \left[\cos \theta \tanh^{-1} \left(\frac{\sin \theta}{\sin \gamma} \right) - \cos \gamma \tanh^{-1} \left(\frac{\sin \theta}{\sin \gamma} \right) \right] + \frac{K(k)}{\pi} \sin 2\theta - \frac{2kK(k)}{\pi} Z(A, k) \cos A \quad (31)$$

where in this case

$$k = \sin \gamma, A = \sin^{-1} \left(\frac{\sin \theta}{\sin \gamma} \right)$$

The angle θ is defined by $\sigma = s_1 e^{i\theta}$ where σ is a point on the circle in the σ plane corresponding to a point on the wing-

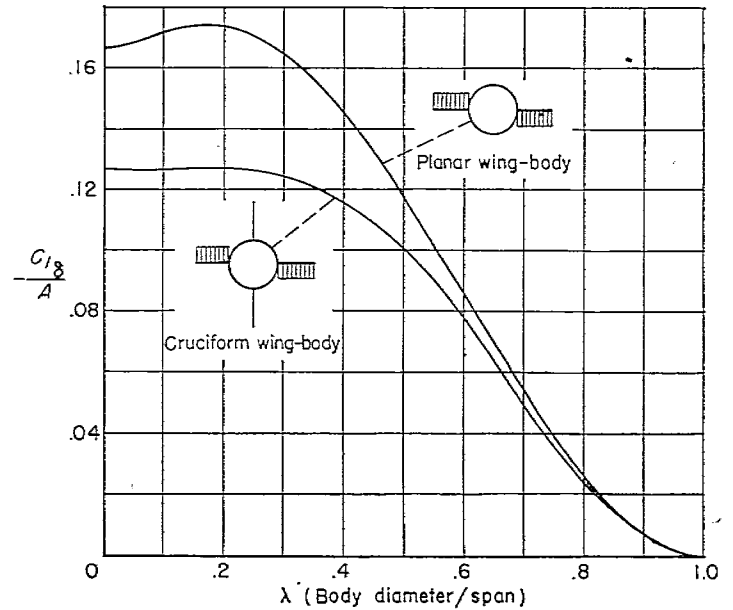


FIGURE 10.—Coefficient of rolling-moment effectiveness for cruciform and planar wing-body combinations with differential incidence of the horizontal surfaces.

body surface in the X plane; the angle γ is the value of θ corresponding to the wing and body juncture. It will be noted that equation (31) is identical in form to equation (18), the potential for the rolling cruciform wing-body combination.

It is seen from figures 9 and 10 that, although the rolling moment supplied by the loading of the deflected surfaces of the cruciform wing-body combination is larger than for the planar wing-body combination, the counter rolling moment induced on the undeflected surfaces reduces the total rolling moment of the former to approximately 75 percent of that for the planar wing-body combination. If both pairs of opposite surfaces of the cruciform wing-body combination are deflected, the rolling moment can be found by the method of superposition to be twice that for one pair, in which case the rolling moment of the cruciform wing-body combination is approximately 1.5 times that of the planar wing-body combination. It can also be seen from these figures that the body has little effect on rolling moment up to a value of $\lambda = 0.3$ for the cruciform wing-body combination.

Equal-span cruciform wing.—If the body radius is set equal to zero (cruciform wing) in equations (27) to (30), the given velocity potentials reduce to

$$\varphi_H = \pm \frac{w_0 s \sqrt{2}}{\pi} [K\sqrt{1 - (y/s)^2} - \sqrt{2}(y/s)KZ(A_7, 1/\sqrt{2})] \quad (32)$$

and

$$\varphi_V = \pm \frac{w_0 s \sqrt{2}}{\pi} \times \{ K\sqrt{1 - (z/s)^2} - \sqrt{2}(z/s)[(E - K)F(A_8, 1/\sqrt{2}) + KE(A_8, 1/\sqrt{2})] \} \quad (33)$$

where

$$A_7 = \cos^{-1}(y/s)$$

$$A_8 = \cos^{-1}(z/s)$$

and the modulus of the elliptic integrals and functions is in all cases $k=1/\sqrt{2}$.

These equations agree with those given in reference 2 for the velocity potentials for a cruciform wing with differential incidence of the horizontal surfaces.

If equations (32) and (33) are substituted in equation (3), it is found that the loading on a spanwise strip of the horizontal surface is

$$P_{H+} = \pm \frac{4\delta\sqrt{2}}{\pi} \frac{ds}{dx} \left[\frac{K + (2E - K)(y/s)^2}{\sqrt{1 - (y/s)^2}} \right]$$

and that the loading on a spanwise strip of the vertical surface is

$$P_{V+} = \pm \frac{4\delta\sqrt{2}}{\pi} \frac{ds}{dx} \left[\frac{K - (2E - K)(z/s)^2}{\sqrt{1 - (z/s)^2}} \right]$$

where $k=1/\sqrt{2}$ in both equations.

Likewise, if the velocity potential² for a planar wing with differential incidence of the wing surfaces is substituted into equation (3), the loading over a spanwise strip obtained is

$$P_- = \pm \frac{8\delta}{\pi} \frac{ds}{dx} \left[\frac{y/s}{\sqrt{1 - (y/s)^2}} \right]$$

Figure 11 shows the loading over the horizontal and vertical surfaces of the cruciform wing in comparison to that over a planar wing when the horizontal wing panels are differentially deflected.

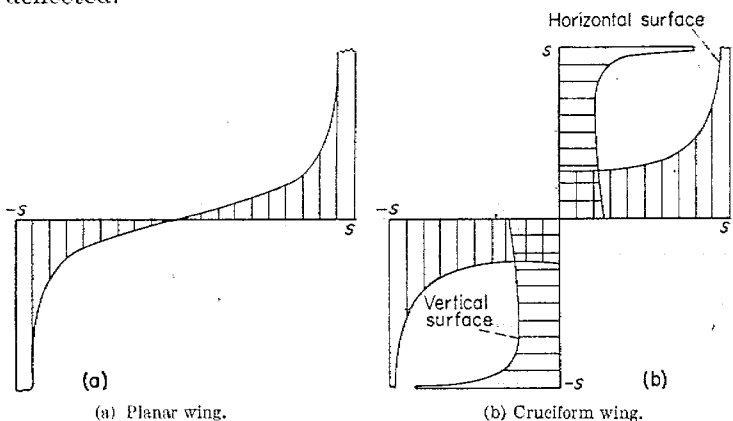


FIGURE 11.—Load distributions on a spanwise strip for wings with differential incidence of the horizontal surfaces.

If the velocity potential for the horizontal surface is substituted into equation (5) and integrated, the rolling moment due to the horizontal surfaces is seen to be

$$\left. \begin{aligned} L'_H &= -\frac{4\sqrt{2}}{3\pi} \left[\frac{K}{2} \left(\frac{\pi}{2} - 1 \right) + E \right] \rho V^2 \delta s_o^3; k=1/\sqrt{2} \\ &= -1.128 \rho V^2 \delta s_o^3 \end{aligned} \right\} (34)$$

Similarly, the rolling moment due to the vertical surface is

$$\left. \begin{aligned} L'_V &= \frac{4\sqrt{2}}{3\pi} \left[\frac{K}{2} \left(\frac{\pi}{2} + 1 \right) - E \right] \rho V^2 \delta s_o^3; k=1/\sqrt{2} \\ &= 0.620 \rho V^2 \delta s_o^3 \end{aligned} \right\} (35)$$

The total rolling moment is therefore

$$\begin{aligned} (L')_+ &= -\frac{4\sqrt{2}}{3\pi} (2E - K) \rho V^2 \delta s_o^3; k=1/\sqrt{2} \\ &= -0.508 \rho V^2 \delta s_o^3 \end{aligned}$$

and the coefficient of rolling-moment effectiveness is

$$\begin{aligned} (C_{l_\delta})_+ &= -\frac{A\sqrt{2}}{3\pi} (2E - K); k=1/\sqrt{2} \\ &= -0.127A \end{aligned}$$

based on the horizontal wing area.

From reference 17, the rolling moment for a slender planar wing having the panels differentially deflected is

$$L' = -0.667 \rho V^2 \delta s_o^3$$

and the coefficient of rolling-moment effectiveness is

$$(C_{l_\delta})_- = -0.167A$$

The ratio of the rolling moments produced by the horizontal panels of the slender cruciform wing and slender planar wing is

$$\frac{(L')_+}{(L')_-} = \frac{2\sqrt{2}}{\pi} (2E - K) = 0.762$$

so that the total rolling moment of the cruciform wing with one pair of opposite panels deflected is 24 percent less than for the planar wing.

If both pairs of surfaces of the cruciform wing were deflected through a small angle δ , the coefficient of rolling-moment effectiveness (based on the horizontal wing area) would be doubled, or

$$(C_{l_\delta})_+ = -0.254A$$

and the total rolling moment would be only 52 percent greater than that of the planar wing.

ROLLING EFFECTIVENESS

A parameter often used in evaluating the rolling effectiveness of a lateral-control system is the rate of change of the wing-tip helix angle $pb_o/2V$ with differential control-surface deflection. This parameter is obtained from the relationship

$$\frac{d}{d\delta} \left(\frac{pb_o}{2V} \right) = \frac{C_{l_\delta}}{C_{l_p}}$$

From the previous results, the helix angle generated by unit incidence of a cruciform wing having four panels equally deflected is

$$\begin{aligned} \left(\frac{C_{l_\delta}}{C_{l_p}} \right)_+ &= \frac{4\sqrt{2}}{3} (2E - K); k=1/\sqrt{2} \\ &= 1.594 \end{aligned}$$

For a planar wing

$$\left(\frac{C_{l_\delta}}{C_{l_p}} \right)_- = 1.696$$

² The velocity potential for this case may be easily derived by applying the Joukowski transformation and the method of this report.

The ratio of the helix angle per unit wing deflection for a cruciform wing to that for a planar wing is therefore

$$\frac{(C_{l_s}/C_{l_p})_+}{(C_{l_s}/C_{l_p})_-} = 0.94$$

It is seen that the rolling effectiveness of a planar wing is reduced 6 percent by the introduction of a wing with identical plan form and surface incidence in the vertical plane of symmetry.

CONCLUSIONS

The application of slender-wing theory to the estimation of the characteristics in roll of slender cruciform wings and wing-body combinations has shown the following:

1. That the damping in roll and the rolling moment due to differential incidence of both pairs of opposite surfaces of the cruciform wing-body combinations are practically independent of the body-diameter-maximum-span ratio up to a value of this ratio of 0.3.

2. That the damping in roll of the cruciform wing-body arrangement is only 62 percent greater than that for a corresponding planar wing-body combination.

3. That the rolling moment, resulting from differential incidence of both pairs of the opposing surfaces of the cruciform wing-body arrangement, is only 52 percent greater than that for a corresponding planar wing-body combination.

4. That the rolling effectiveness (wing-tip helix angle per unit surface deflection) of the cruciform wing-body arrangement having four equally deflected panels is therefore 94 percent of the corresponding planar wing-body combination.

It is of interest to point out that the method of analysis may be applied to the investigation of the characteristics of slender cruciform wing-body combinations which have any specified distribution of normal velocity on the surfaces of the wings and body.

AMES AERONAUTICAL LABORATORY.

NATIONAL ADVISORY COMMITTEE FOR AERONAUTICS,
MOFFETT FIELD, CALIF., Sept. 29, 1950.

REFERENCES

1. Spreiter, John R.: The Aerodynamic Forces on Slender Plane- and Cruciform-Wing and Body Combinations. NACA Rep. No. 962, 1950. (Formerly NACA TN's 1662 and 1897)
2. Adams, Gaynor J.: Theoretical Damping in Roll and Rolling Effectiveness of Slender Cruciform Wings. NACA TN 2270, 1951.
3. Ribner, Herbert S.: Damping in Roll of Cruciform and Some Related Delta Wings at Supersonic Speeds. NACA TN 2285, 1951.
4. Bleviss, Zegmund O.: Some Roll Characteristics of Plane and Cruciform Delta Ailerons and Wings in Supersonic Flow. Douglas Rep. No. SM-13431, 1949.
5. Graham, Ernest W.: A Limiting Case for Missile Rolling Moments. Jour. Aero. Sci., Sept. 1951, pp. 624-628.
6. Tucker, Warren A., and Piland, Robert O.: Estimation of the Damping in Roll of Supersonic-Leading-Edge Wing-Body Combinations. NACA TN 2151, 1950.
7. Jones, Robert T.: Properties of Low-Aspect-Ratio Pointed Wings at Speeds Below and Above the Speed of Sound. NACA Rep. 835, 1946. (Formerly ACR L5F13, and NACA TN 1032)
8. Heaslet, Max. A., Lomax, Harvard, and Spreiter, John R.: Linearized Compressible-Flow Theory for Sonic Flight Speeds. NACA Rep. 956, 1950. (Formerly TN 1824)
9. Lomax, Harvard, and Heaslet, Max. A.: Linearized Lifting-Surface Theory for Swept-Back Wings With Slender Plan Forms. NACA TN 1992, 1949.
10. Darwin, Sir Charles: Some Conformal Transformations Involving Elliptic Functions. Philosophical Magazine, vol. 41, ser. 7, no. 312, Jan. 1950, pp. 1-11.
11. Westwater, F. L.: Some Applications of Conformal Transformation to Airscrew Theory. Proc. Cambridge Phil. Soc., vol. 32, 1936, pp. 676-684.
12. Lomax, Harvard, and Heaslet, Max. A.: Damping-in-Roll Calculations for Slender Swept-Back Wings and Slender Wing-Body Combinations. NACA TN 1950, 1949.
13. Ribner, Herbert S.: A Transonic Propeller of Triangular Plan Form. NACA TN 1303, 1947.
14. Whittaker, E. T., and Watson, G. N.: A Course of Modern Analysis. The Macmillan Company, New York, 1947.
15. King, Louis V.: On the Direct Numerical Calculation of Elliptic Functions and Integrals. Cambridge, England, University Press, 1924.
16. Heuman, Carl: Tables of Complete Elliptic Integrals. Jour. Math. and Physics, vol. 19-20, 1940-41, pp. 127-142.
17. DeYoung, John: Spanwise Loading for Wings and Control Surfaces of Low Aspect Ratio. NACA TN 2011, 1950.